Asian Journal of Information Technology 13 (9): 477-484, 2014
ISSN: 1682-3915

A New Automated CAD System for Classification of Malignant and Benign Lesions

Norhene Gargouri Ben Ayed, Alima Damak Masmoudi and Dorra Sellami Masmoudi
Sfax Engineering School, Computers Imaging Electronicsand Systems Group (CIELS),
University of Sfax, Sfax, Tunisia

Abstract: This study presents a completely automated Computer-Aided Diagnostic (CAD) System for mass detection, segmentation and classification. This system performs mass detection followed by the classification as benign-malignant on the detected and segmented masses. In order to make mass detection more effective, a sequence of preprocessing steps are designed for contrast enhancement and noise effects removal as well as the effectiveness of the stage of detection. The location of suspicious masses using a new approach named Improved Against Noise Gray Level and Local Difference (IANGLLD) is developed for mass texture extraction. As the shapes of masses are fundamental in the classification between benignancy and malignancy, two shape features are used and joined with the texture features applied in mass detection to be the input of the ANN for mass classification. For the evaluation of the proposed system the Digital Database for Screening Mammography (DDSM) was applied to evaluate the performance. The obtained results are encouraging and have revealed promise of the proposed system.

Key words: CAD, IANGLLD, mass texture extraction, digital database, DDSM

INTRODUCTION

Although, mammography is considered as the most effective screening method for breast cancer diagnosis, this later is based on radiologist's personal experiences. Studies have shown that the diagnosis can at most achieve 85% accuracy. Generally, radiologists ask the patient to do biopsies as final diagnosis. To overcome these problems, it is so important to use the computer-aided system (Vyborny, 1994).

Few researchers have recently developed different approaches to accomplish the detection and classification of masses. Lai *et al.* (1989), applied image enhancement and template matching in order to detect masses. The disadvantage of this method is that it is limited to circumscribed masses. Brzakovic *et al.* (1990), applied on the extracted ROIs, the thresholding and fuzzy pyramid linking algorithm for the segmentation and detection of masses. Depending on extracted morphological feature of segmented objects they classify masses as benign, malignant or non tumor. In 85% of the cases a correct classification was achieved.

In order to decide about the location of masses, some researchers (Yin *et al.*, 1991) had proposed the employment of the asymmetry of the two sides of the breast. Texture features were used for the differentiation between masses and non-masses. Kegelmeyer *et al.* (1994) used texture features and edge characteristics for the detection of speculated masses. Chan *et al.* (1995) and Wei *et al.* (1995) used texture features and linear discrimination to differentiate between masses and non masses. Christoyianni *et al.* (2000) proposed the computer aided system for identification of circumscribed mass.

Automatic mass detection and segmentation in mammograms are still considered as challenging problems. Generally, the masses mix with the normal tissues, the gray levels may vary with the distribution of the breast (De Paredas, 1994). In some cases, the intensity of the breast background is higher than the intensity of the masses causing minimum detection before segmentation.

Although, almost the density and the gray levels of the opacities are higher than the normal tissue, some masses have unclear boundary. In other cases, the contrast between edges of the masses and backgrounds is low or masses may be covered by the background tissue that's why, the difficulty of masses detection increases. Figure 1 illustrates an example where the region in the square has been proven as a mass, however this cannot be observed from the digitized mammogram. In such example, the mass cannot be detected by using only segmentation method as proposed by some researchers (Kegelmeyer *et al.*, 1994). Texture features variation is

Corresponding Author: Gargouri Ben Ayed, Sfax Engineering School, Computers Imaging Electronicsand Systems Group (CIELS), University of Sfax, Sfax, Tunisia

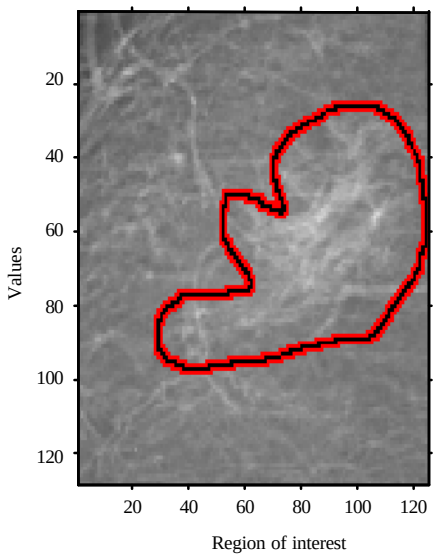

Fig. 1: Example of interest region of mammogram from DDSM database

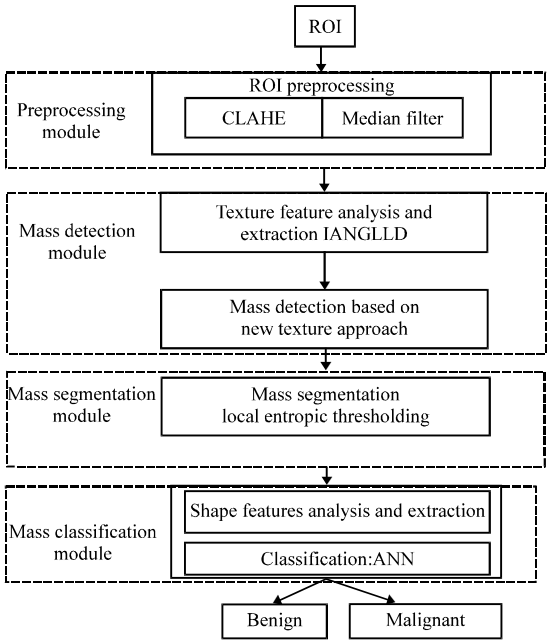

Fig. 2: System diagram

more reliable than the variation of the gray levels or the variation the contrast of the intensities for mass detected (Bovis and Singh, 2000; Sameti *et al*., 1997). Based on this consideration, researchers propose a system using texture for mass detection.

The texture features adopted are the improved gray level and local difference (Gargouri *et al*., 2012). Due to the excellent performance proved by the Gray Level and Local Difference (GLLD), researchers propose in this research to improve its performance in order to achieve better results. The major problem in the task of mass classification is caused by the diversity in features. In fact, very diverse signs of abnormality are observed by the expert radiologists. In the last decade, some researcher's template are developped in order to code geometric structures for specific category of masses. Then, they combined those templates from a digitized mammogram. Based on this approach, they are limited to just specific category of masses. The Artificial Neural Networks (ANN) are regarded all these years as the most prominent tool for classification of such systems. This later is based on the imitation of the neurons in human beings by using a simple correction of artificial neurons. The neural network has a high copy of parallel computing and has robust resemblance ability. Beacause of the afore-mentioned reasons, the texture features are considered, in the proposed system as input of the ANN for the classification stage.

Shape features are among the most prominent features applied for the differentiation between malignant and benign masses. So, it will be used for mass classification. In fact, the obtained accuracy of segmentation affects the stage of shape features extraction. The results obtained from the ANN are not sufficient for shape calculation. Consequently, researchers propose to apply Entropic Thresholding Methods form the mass segmentation stage in order to obtain fine-segmentation mass. The proposed fine segmentation which is proposed will be applied only on the detected area in the detection stage allows to reduce the noise caused from the background. In the final step, two different shape features were applied to the neural network system for the classification of the masses as malignant or benignant. The diagram of the proposed system is illustrated in Fig. 2. In the Region of Interest (ROI) preprocessing module, the ROI undergoes a preprocessing stage to overcome the problem of noise and enhance the features. Then, the IANGLLD are used as features of the image.

The obtained features are then classified as mass or non-mass using the ANN. The mass segmentation module is then applied to segment masses by applying Local Entropy Method. The mass region are finally after segmentation stage classified as benign or malignant by applying the ANN with inputs of texture and shape features corresponding to the segmented mass.

ROI preprocessing: Researchers propose, in this study, two-stage process based on Contrast Limited Adaptative Histogram Equalization (CLAHE) and median filter. The ROIs are generally very small; they correspond to the area being considered as suspicious region.

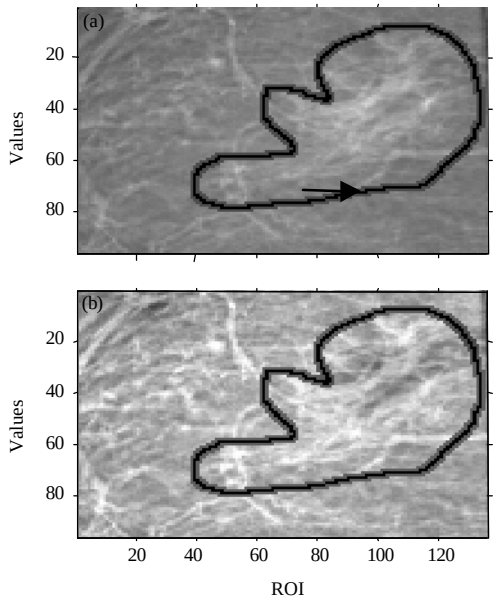

Fig. 3: Example of enhancement of a ROI by CLAHE; a) original ROI; b) ROI after contrast enhancement

Adaptative Histogram Equalization (AHE): The AHE allows contrast enhancement. This approach divides the image into small regions called tiles and then stretches the histogram for each tiles allowing its adjustement in area having non uniform distribution. This technique treats early parts of the image then combines them using bilinear interpolation to reduce edge effects.

Contrast Limited Adaptative Histogram Equalization (CLAHE) for contrast enhancement: This approach is an improved technique of the AHE. It allows to improve the visibility of local details in an image by increasing its contrast in local areas (Pizer *et al*., 1990). As a result, a cumulative histogram is built from the histogram clipping. The effect of this clipping on the histogram is presented on a mammogram image from Digital Database on Screening Mammography (DDSM) as it is shown in Fig. 3.

Removal of noise effects: In the previous stage, the contrast of the image was enhanced. However, noise pixel presents a limitation. To cope with this dilemma, researchers propose to apply the median filter. These noise pixels are removed by:

$$I_2(x,y) = \text{Median}\{I_1(x,y)\} \quad (1)$$

$$I_2(x,y) = \text{Median}\left\{\sum_{i=-1}^{1}\sum_{j=-1}^{1} I_1(x+i,y+j)\right\} \quad (2)$$

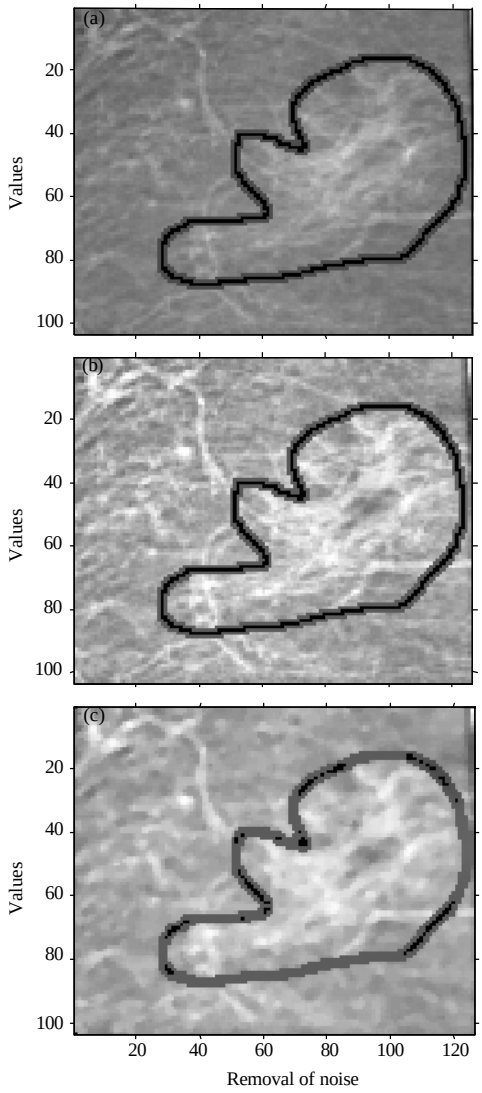

Fig. 4: ROI preprocessing; a) original ROI; b) ROI after contrast enhancement; c) ROI after contrast enhancement end removal of noise effects

The median filter is based on the use of 3×3 windows. Figure 4 shows the results of the application of the median filter to the enhanced image in Fig. 3. The noise pixels in general have correlation with the mass pixels; the application of the median filter may smooth out these pixels and reduce their effects.

Noise Robust Automatic Detection Method: After the stage of ROI extraction, the next phase is masses segmentation. In fact, features of masses present different features for the textures of normal tissues. A new approach is developed in this study for the stage of feature extraction.

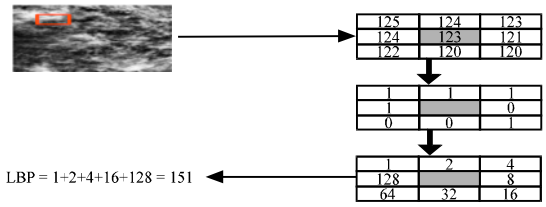

Fig. 5: Example of basic LBP operator

Brief review of LBP formulation: The LBP operator uses the eight neighboring pixels and considers the center gray value as the threshold value. This operator is defined as in Fig. 5. Referring to Fig. 5, LBP (Ojala *et al*., 2001) code could be computed as follows:

$$LBP_{P,R} = \sum_{p=0}^{P-1} s(g_p - g_c) \quad (3)$$

$$S(x) = \begin{cases} 1 & si\ x \geq 0 \\ 0 & si\ x < 0 \end{cases} \quad (4)$$

Where:

g_c = The gray value of the central pixel
g_p = The value of its neighbors (p = 0, 1,..., P-1)
P = Number of neighbors
R = Radius of the neighborhood

The obtained binary code is, then, represented with a 8 bit number. The coordinates of g_p are ((Rcos(2.pi.p/P), Rsin(2.pi.p/P)).

Against noise gray level and local difference feature based approach: The major limitation with LBP code is that it may present the same outcome with two completely dissimilar gray levels as the differences with the same neighbors.

In fact, for mammographic images, the gray level information is related to the breast tissue. Therefore, gray level and local difference are considered as two important features of the texture which must be used together in order to have more accurate results.

Kegelmeyer *et al.* (1994), had proposed the GLLD approach as texture feature descriptor. In his approach researchers compute the average for each 3×3 neighborhood and attribute it to the central pixel. The novel value of this later is noted as g_{cmean}. Feature extraction is the more important task for decision about malignancy of mammographic masses. To improve the detection rate, a new feature against noise named ANGLLD (Against Noise Gray level and Local Difference) is developed for texture feature extraction.

The obtained vector of the difference is decomposed of sign and modulus components. $Diff_p = mean_p - g_{cmean}$, $mean_p$ is set as the mean value of the pth 3×3 window elements, s_p corresponds to the sign of differences as defined in Eq. 5. However, m_p corresponds to the modulus of $diff_p$ as expressed in Eq. 6:

$$s_p = s(diff_p) \quad (5)$$

$$m_p = |diff_p| \quad (6)$$

The value of the central pixel which corresponds to the mean value of its neighbors could also give useful information (Gargouri *et al*., 2012). The fusion by concatenation of the sign, the modulus and the central gray level codes provide better performance than each code (Gargouri *et al*., 2012). Given a pixel in the mammographic image, the sign component is noted as SANGLLD and is computed as follows:

$$SANGLLD_{P,R} = \sum_{p=0}^{P-1} s(mean_p - g_{cmean}) 2^p \quad (7)$$

The coding of the magnitude component MANGLLD is defined as follows:

$$MANGLLD_{P,R} = \sum_{p=0}^{P-1} t(m_p, c) 2^p \quad (8)$$

$$t(x,c) = \begin{cases} 1 & x \geq c \\ 0 & x < c \end{cases} \quad (9)$$

where, c represents a global gray level threshold and is determined adaptively. It is set as the average value from the image. The value of the central pixel represents discriminant information. It is coded as:

$$CANGLLD_{P,R} = t(g_{cmean}, c_I) \quad (10)$$

where, t defined in Eq. 10, c_I represents the threshold and is considered as the mean gray level of the whole image.

IANGLLD feature: The main limitation using GLLD code (Gargouri *et al*., 2012) is that the obtained code is of large size. Knowing that the size of the input vector at the classification stage affects in the choice of the classifier. For example, the ANN based in radial basis functions cannot be adopted in the case of input vector of large size. So, researchers propose to apply another method for the fusion of the three operators. The proposed technique consists in combining the obtained operators SANGLLD, MANGLLD and CANGLLD in an hubrid way. In this way, first a 2D joint histogram, "S/CANGLLD" or

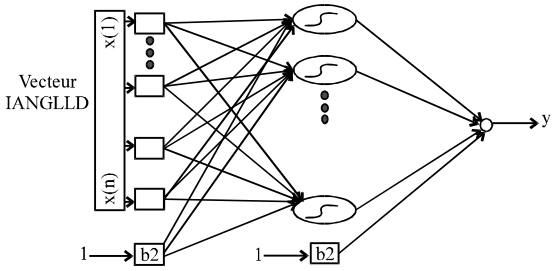

Fig. 6: Architecture of ANN

"M/CANGLLD" is built, then this histogram is transformed to a 1D histogram. The later is a second time concatenated with MANGLLD or SANGLLD to produce the joint histogram, denoted by "M_S/CANGLLD" or "S_M/CANGLLD".

The obtained features are applied to the ANN, to train the ANN for mass detection. The ANN architecture is illustrated in Fig. 6.

Mass segmentation: According to the obtained result in study, the regions in the ROIs can be segmented as masses, background and edges. The segmentation of masses is carried out applying the Entropic Thresholding Method.

Let, G = {0, 1, L-1} be the gray level range and t the threshold which allow the partition of the gray levels G into the regions G0 = {0, 1, 2, ..., t} and G1 = {t, t+1, ..., L-1}. The obtained matrix W from the IANGLLD when thresholded by t may be divided into four different quadrants:

- Background to Background (BB)
- Foreground to Background (FB)
- Foreground to Foreground (FF)
- Background to Foreground (BF)

The pixels corresponding to the gray levels above t are considered foreground otherwise they are considered as background.

Assuming that the probability corresponding to the four quadrants are: $P_{BB}(i, j)$, $P_{BF}(i, j)$, $P_{FB}(i, j)$ and $P_{FF}(i, j)$ (Liao *et al.*, 1996), the entropies corresponding to these different quadrants may be defined as follows:

$$H_{BB}(t) = -\sum_{i=0}^{t}\sum_{j=0}^{t} P_{BB(i,j)} \log P_{BB(i,j)} \quad (11)$$

$$H_{BF}(t) = -\sum_{i=0}^{t}\sum_{j=t+1}^{L-1} P_{BF(i,j)} \log P_{BF(i,j)} \quad (12)$$

$$H_{FB}(t) = -\sum_{i=t+1}^{L-1}\sum_{j=0}^{t} P_{FB(i,j)} \log P_{FB(i,j)} \quad (13)$$

$$H_{FF}(t) = -\sum_{i=t+1}^{L-1}\sum_{j=t+1}^{L-1} P_{FF(i,j)} \log P_{FF(i,j)} \quad (14)$$

BB and FF correspond to the translations of the gray level between background and foreground and between foreground to foreground, respectively consequently they correspond to local properties and they may be defined as:

$$H_{LE}(t) = H_{BB}(t) + H_{FF}(t) \quad (15)$$

So, local entropy is defined. In the same manner, BF and FB corresponds to joint properties, so the joint entropy can be defined as:

$$H_{JE}(t) = H_{BF}(t) + H_{FB}(t) \quad (16)$$

Therefore, the local threshold indicated by t_{LE} maximizes the equation of the local entropy, similarly, the threshold indicated by t_{JE} maximizes the joint entropy and they are defined as follows:

$$t_{LE} = \arg\{\max_t H_{LE}(t)\} \quad (17)$$

$$t_{JE} = \arg\{\max_t H_{JE}(t)\} \quad (18)$$

Based on the results presented by Pal and Pal (1989), may choose the local entropy to the purpose.

Diagnosis of malignant and benign criteria and analysis of shape feature: After mass detection and segmentation, it is primordial to classify the mass as malignant or benign.

Diagnosis criteria

Malignancy criteria:

- In general, speculated masses are considered as the most obvious basis for the decision of early malignancy
- The density is generally high in the case of malignant mass
- In the case of the edge of the mass in one side obscure and in another side very clear, it may be malignant
- In the case of two views of the breast have assymetrical density, it may be malignant
- If masses present nodes on the edge, it may be malignant

Benignancy criteria:

- If the mass corresponds to fibroadenoma or benign macrocyst, it is benign
- In the case of circumscribed masses, it is usually benign

Shape feature extraction: Texture and shape features are two important features for discrimination between masses according to their degree of malignity. Researchers will introduce, in this study, two shape descriptors including circularity and radial angle. These descriptors will be used on the obtained segmented mass for shape feature extraction.

Circularity: The main function of circularity is to illustrate the degree of circularity of masses (Petrick *et al*., 1996). The high circularity indicates that the object is circular. The roundness is one of the most important criteria of benignity; the probability of masses to be benign is higher when the circularity is higher.

Let, R be the region of masses. In the calculation of the mass circularity, if a circle C_{eq} has the same area as the segmented mass, its center corresponds to the center of the mass. The overlapping ratio of the obtained circle and the segmented mass is calculated as the circularity. The equations allowing calculating the circularity are presented from Eq. 20-24 as:

$$S = \sum_{(x,y)\in R} 1 \tag{19}$$

S corresponds to the area of the segmented mass. The center of this mass noted as $(\bar{x}, \bar{y})$ is defined by:

$$\bar{x} = \frac{1}{S}\sum_{(x,y)\in R} x \tag{20}$$

$$\bar{y} = \frac{1}{S}\sum_{(x,y)\in R} y \tag{21}$$

And the radius R_{eq} of the circle C_{eq} is defined by:

$$R_{eq} = \sqrt{\frac{area(C_{eq})}{\pi}} = \sqrt{\frac{area(R)}{\pi}} = \sqrt{\frac{S}{\pi}} \tag{22}$$

The circularity can be computed as follows:

$$Circularity = \frac{Area(R \cap C_{eq})}{Area(R)} \tag{23}$$

The value of the circularity would be between 0 and 1. If the ratio is 1, the mass is circular. If the circularity is smaller than 1, the mass is not a circle.

Contrast: Generally, the intensities corresponding to malignant masses are higher than the intensities of benign masses. In addition, the contrast of masses with respect to their background is higher than this of benign masses.

The contrast is calculated as a difference between the average of the gray level of masses and that of tissue within a defined ring-like operator. The ring like operator is expressed as:

$$\Omega = \left\{(x,y)\middle| d \le \sqrt{x^2 + y^2} \le d + \Delta d\right\} \tag{24}$$

D corresponds to the radius. This later is the smallest circle which contains the mass, Δd corresponds to the width of the ring-like operator. The Δd is set as 5. The contrast is calculated as follows: R corresponds to the region of masses.

RESULTS

For the evaluation of the performance of the module of mass detection, let's consider N_p the total number corresponding to positive ROI's and N_n is the total number of negative ROIs. Researchers define then the TPN as the number of detected ROIs containing masses and FPN the number of ROIs containing no masses but are detected as masses. The True Negative Number (TNN) and the False Negative Number (FNN) may be defined as TNN = N_n-FPN and FNN = N_p-TPN, respectively. In the evaluation, for mass detection, 100 masses and 600 textures were applied for training and 60 masses and 400 textures were used for test. The mass contours are delineated by radiologists and used as the ground truth for mass detection. The ROIs inside the contour of the masses are considered as masses, however, outside the contour of mass, they are considered texture.

For the evaluation of the proposed system, the Receiver Operating Characteristics (ROC) was applied to evaluate the performance and the area under curve, AUC is applied as a measure indicator. The larger the AUC is the higher the obtained performance will be.

The detection accuracy results is shown in Table 1. From the obtained results, it may be observed that the IANGLLD approach achieves better results (98%) than the other methods in comparison. Furthermore, in the obtained experimental results, it is observed that the ANN classifier is better than the SVM classifier. These results demonstrates the good performance even in difficult cases.

Table 1: Detection accuracy (%) for 1000 samples uniformly distributed for test and training from the DDSM database

Methods	Classifier	Accuracy
LBP	ANN	96.1
	SVM	94.5
GLLD	ANN	98.2
	SVM	93.0
IANGLLD	ANN	98.9
	SVM	92.5

Table 2: AUC of the different features used for masses detection classification

Feature types	Feature	AUC	Averaged AUC
Texture feature	IANGLLD	0.96	0.82
Shape feature	Contrast	0.74	
	Circularity	0.72	

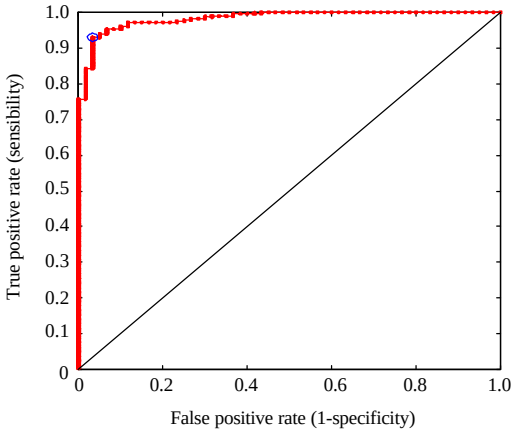

Fig. 7: ROC curve

Table 2 illustrates the AUC value for texture feature and each single shape feature. The fourth column illustrates the average of the AUC values corresponding to shape features, however the fifth column is reserved to the average AUC value for all the proposed features. From the obtained results in Table 2, researchers can see that the contrast shows better performance with 0.76 of the AUC value. Additionally, the texture feature has higher AUC value (0.96) than the shape feature. The total AUC value corresponding to the average value is 0.82.

As result of the final experiment, the system takes all obtained features as input vector to the ANN for the stage of classification. Figure 6 shows the diagram of the ANN classification module. In this later, the input vector was the 2 shape features and the texture features. The 50 ROIs were used as training patterns including 25 malignant masses and 25 benign masses and 50 ROIs were used for testing including 25 malignant masses and 25 benign masses. The ROC curve is plotted in Fig. 7 where the AUC is equal to 0.98. Obviously, integrating all the features as input of the ANN for classification demonstrates higher performance than applying each feature separately in Table 1.

CONCLUSION

In this study, a computer-aided system for detection, segmentation and classification of opacities presented. It is based on a preprocessing with IANGLLD for detection of masses and the entropic thresholding for the stage of segmentation. The preprocessing is designed for enhancement of the contrast of the masses and the elimination of the noise effects. In order to detect masses, the ANN was applied to achieve the classification. The local entropy thresholding is based on the extraction of masses to obtain the shape of the masses. In fact, the shape of masses is an important aspect for discrimination of the masses benignancy or malignancy. Finally, the ANN was applied again for classification of masses. The experimental results show that the integration by ANN is so important for classification of masses.

The proposed system was composed of four modules: mammogram preprocessing, masses detection, masses segmentation and masses classification where each stage performs a specific task, it can be improved individually in the future. For evaluation of the proposed system, a data set of the DDSM database was used for the training and the test. The results for such system illustrates that the proposed system performs well and has great promise in clinical applications.

ACKNOWLEDGEMENT

Researchers would like to thank Dr. Abid Riadh, Radiologist at El Farabi Imaging Center, Sfax, Tunisia and at the Faculty of Medecine of Sfax for this helpful discussions and advices. Researchers want also to thank MVG and VGG for sharing their source codes of LBP.

REFERENCES

Bovis, K. and S. Singh, 2000. Detection of masses in mammograms using texture features. Proceedings of the 15th International Conference on Pattern Recognition, Volume 2, September 3-7, 2000, Barcelona, pp: 267-270.

Brzakovic, D., X.M. Luo and P. Brzakovic, 1990. An approach to automated detection of tumors in mammograms. IEEE Trans. Med. Imaging, 9: 233-241.

Chan, H.P., D. Wei, M.A. Helvie, B. Sahiner, D.D. Adler, M.M. Goodsitt and N. Petrick, 1995. Computer-aided classification of mammographic masses and normal tissue: Linear discriminant analysis in texture feature space. Phys. Med. Biol., 40: 857-876.

Christoyianni, I., E. Dermatas and G. Kokkinakis, 2000. Fast detection of masses in computer-aided mammography. Signal Process. Mag., 17: 54-64.

De Paredas, E.S., 1994. Radiographic breast anatomy: Radiologic signs of breast cancer. RSNA Categorical Course Phys., 1: 35-46.

Gargouri, N., A.D. Masmoudi, D.S. Masmoudi and R. Abid, 2012. A new GLLD operator for mass detection in digital mammograms. J. Biom. Imaging, Volume 2012. 10.1155/2012/765649.

Kegelmeyer Jr, W.P., J.M. Pruneda, P.D. Bourland, A. Hillis, M.W. Riggs and M.L. Nipper, 1994. Computer-aided mammographic screening for spiculated lesions. Radiology, 191: 331-337.

Lai, S.M., X. Li and W.F. Biscof, 1989. On techniques for detecting circumscribed masses in mammograms. IEEE Trans. Med. Imaging, 8: 377-386.

Liao, P.S., B.C. Hsu, C.S. Lo, P.C. Chung and T.S. Chen *et al*., 1996. Automatic detection of microcalcifications in digital mammograms by entropy thresholding. Proceeding of the 18th Annual International Conference of the IEEE Engineering in Medicine and Biology Society, October 31-November 3, 1996, Amsterdam, pp: 1075-1076.

Ojala, T., K. Valkealahti, E. Oja and M. Pietikainen, 2001. Texture discrimination with multidimensional distributions of signed gray-level differences. Pattern Recogn., 34: 727-739.

Pal, N.R. and S.K. Pal, 1989. Entropic thresholding. Signal Process., 16: 97-108.

Petrick, N., H.P. Chan, B. Sahiner and D. Wei, 1996. An adaptive density-weighted contrast enhancement filter for mammographic breast mass detection. IEEE Trans. Med. Imag., 15: 59-67.

Pizer, S.M., R.E. Johnston, J.P. Ericksen, B.C. Yankaskas and K.E. Muller, 1990. Contrast-limited adaptive histogram equalization: Speed and effectiveness. Proceedings of the 1st Conference on Visualization in Biomedical Computing, May 22-25, 1990, Atlanta, GA., pp: 337-345.

Sameti, M., R.K. Ward, B. Palcic and J. Morgan-Parkes, 1997. Texture feature extraction for tumor detection in mammographic images. Proceedings of the IEEE Pacific Rim Conference on Communications, Computers and Signal Processing, Volume 2, August 20-22, 1997, Victoria, BC., pp: 831-834.

Vyborny, C.J., 1994. Can computers help radiologists read mammograms. Radiology, 191: 315-317.

Wei, D., H.P. Chan, M.A. Helvie, B. Sahiner, N. Petrick, D.D. Adler and M.M. Goodsitt, 1995. Classification of mass and normal breast tissue on digital mammograms: Multiresolution texture analysis. Med. Phys., 22: 1501-1513.

Yin, F.F., M.L. Giger, K. Doi, C.E. Metz, C.J. Vyborny and R.A. Schmidt, 1991. Computerized detection of masses in digital mammograms: Analysis of bilateral subtraction images. Med. Phys., 18: 955-963.